Desymmetrized Vertex Design for the Synthesis of Covalent Organic Frameworks with Periodically Heterogeneous Pore Structures

Youlong Zhu,[†] Shun Wan,[‡] Yinghua Jin,[†] and Wei Zhang*,[†]

[†]Department of Chemistry and Biochemistry, University of Colorado, Boulder, Colorado 80309, United States
[‡]Storagenergy Technologies, Inc., Salt Lake City, Utah 84120, United States

S *Supporting Information*

ABSTRACT: Two novel porous 2D covalent organic frameworks (COFs) with periodically heterogeneous pore structures were successfully synthesized through desymmetrized vertex design strategy. Condensation of C_{2v} symmetric 5-(4-formylphenyl)isophthalaldehyde or 5-((4-formylphenyl)ethylene)isophthalaldehyde with linear hydrazine linker under the solvothermal or microwave heating conditions yields crystalline 2D COFs, **HP-COF-1** and **HP-COF-2**, with high specific surface areas and dual pore structures. PXRD patterns and computer modeling study, together with pore size distribution analysis confirm that each of the resulting COFs exhibits two distinctively different hexagonal pores. The structures were characterized by FT-IR, solid state ^{13}C NMR, gas adsorption, SEM, TEM, and theoretical simulations. Such rational design and synthetic strategy provide new possibilities for preparing highly ordered porous polymers with heterogeneous pore structures.

In the past decade, covalent organic frameworks (COFs)[1−8] have emerged as a new class of highly ordered crystalline organic porous polymers and have attracted tremendous research interests due to their unique structures and various potential applications in gas storage and separation,[9,10] heterogeneous catalysis,[11,12] optoelectronic materials,[13,14] and energy storage.[15] COFs are constructed through reticular synthesis[16] involving dynamic covalent reactions[17] in solution or on surface.[18,19] Such approach provides precise periodicity control in skeleton, customizable pore surface, and structural diversity as well as high physiochemical stability. A large number of COFs have been synthesized and characterized within the past decade. However, they are mainly limited to uniform pore structures with homogeneous pore environments. Introduction of pore heterogeneity within ordered COFs is desirable to tailor materials characteristics, such as electronic, magnetic, mechanical, and sorption properties. Structural disorders and heterogeneities have been widely investigated in hierarchical porous polymers (HPPs)[20−22] and metal–organic frameworks (MOFs),[23−28] which have shown intriguing applications in catalysis and separation technology. In most cases, such structural "defects" are randomly distributed, and their spatial arrangements are hard to identify. Complex COFs with intentionally created heterogeneities are rare.[29−32] One such example was recently reported by Zhao et al., demonstrating the synthesis of a 2D COF with dual pores.[29]

Our group also attempted to prepare COFs with dual pores through "macrocycle-to-framework" strategy using a preporous shape-persistent macrocycle as a building block.[31] However, due to the small internal cavity of the macrocycle, it was difficult to identify and characterize the small pores. Herein we describe a facile and conceptual approach which can produce COFs with predesigned periodic "defects" in the ordered framework.

Conventionally, COFs are synthesized from highly symmetric building blocks in order to form well-ordered, easily predictable crystalline structures. Multitopic building blocks with C_3/D_{3h} or C_4/D_{4h} symmetry are the most commonly used.[33] By using these types of building blocks as vertices along with ditopic linear linkers, the extended topological structures with high symmetry can be achieved. Such approach creates COFs with uniform pore structures (e.g., hexagonal or tetragonal). We envision that introducing asymmetric elements into building block design could create COFs with heterogeneous pore structures (HP-COFs). For example, desymmetrization of a D_{3h} vertex to C_{2v} would generate a 2D framework structure possessing two different hexagonal pores, as shown in Scheme 1.

Following the desymmetrized vertex design strategy, we designed and synthesized C_{2v} symmetric 5-(4-formylphenyl)-

Scheme 1. Design Strategy for the Synthesis of HP-COFs
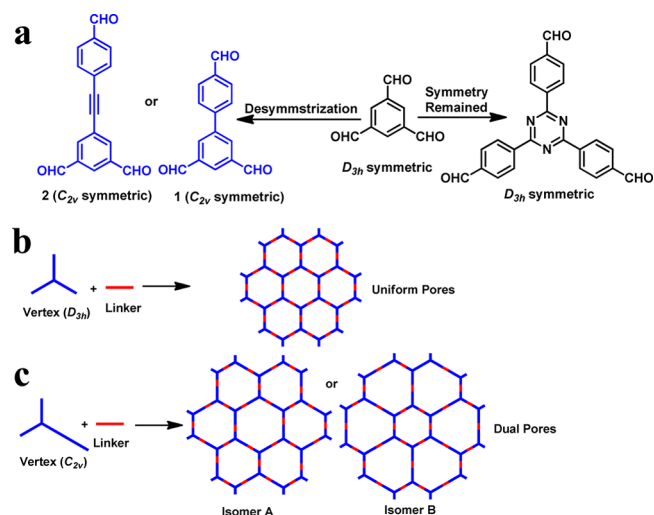
isophthalaldehyde (**1**) and 5-((4-formylphenyl)ethylene)-isophthalaldehyde (**2**) as the tritopic vertex to form 2D covalent organic frameworks with two different kinds of hexagonal honeycomb pores. We chose hydrazine, which is the smallest diamine, as the ditopic linear linker to amplify the pore size difference. In addition, condensation of hydrazine and aldehydes can form diazabutadiene (−C=N−N=C−) linkages, which have been reported to be stable in water, acidic media, and basic media.[34] The reaction was carried out under solvothermal conditions by using 1,4-dioxane and 1,2-dichlorobenzene (*o*-DCB) as the cosolvents in the presence of acetic acid (6 M). We screened the synthetic conditions by varying the solvent combination/ratio, reaction temperature/time, and catalyst loading in order to optimize the porosity and crystallinity of the materials. Under the optimal synthetic condition, 10/5/1 (v/v/v) ratio of 1,4-dioxane, *o*-DCB, and 6 M acetic acid at 150 °C for 4 days, we obtained HP-COF-1 and HP-COF-2 as light-yellow microcrystalline solids. As an alternative approach, the microwave heating method[35,36] was also utilized to synthesize both COFs, which show similar powder X-ray diffraction (PXRD) patterns as those obtained under solvothermal conditions. The resulting HP-COFs are stable in common organic solvents, such as dimethylformamide (DMF), tetrahydrofuran (THF), chloroform, acetone, and dichloromethane.

The as-synthesized HP-COFs were characterized by Fourier transform infrared spectroscopy (FT-IR). The spectra of HP-COFs show the nearly complete disappearance of C=O resonance, indicating the aldehydes are mostly consumed during the reaction. In addition, the strong stretching vibration band at 1622 cm^{-1} was observed, confirming the formation of C=N linkage (Figure S2). The ^{13}C CP-MAS NMR spectrum shows the characteristic signal for the C=N group at about 161 ppm. The aldehyde carbon peak was barely observed. The chemical shifts of other fragments are in good agreement with those of the monomers (Figure S21 and S22). Thermal gravimetric analysis (TGA) reveals that the HP-COF-1 and HP-COF-2 are stable up to 300 °C, with around 20% weight loss at 400 °C (Figure S1). Field emission scanning electron microscopy (FE-SEM) images show that both COFs have sponge-like morphologies (Figure S23 and S24). Transmission electron microscopy (TEM) characterization reveals their layered structures with the interlayer distance around 3.45 Å (Figure 1). Our observation is consistent with the previous literature report,[1,7,8,15,37,38] supporting the 2D nature of these frameworks.

The porosity of each COF was assessed by measuring N$_2$ adsorption/desorption isotherms at 77 K on the fully activated samples. The adsorption curves of HP-COFs (Figure 3a) show typical type I isotherm according to the IUPAC notation,[39] which is the characteristic of microporous materials. Employing the Brunauer−Emmett−Teller (BET) model over the $0.01 \leq P/P_0 \leq 0.10$ range of the isotherms, we obtained a specific surface area of 1197 m^2 g^{-1} for HP-COF-1 and 804 m^2 g^{-1} for HP-COF-2, which are comparable to that of the recently reported azine-based COFs.[34,40] The total pore volumes of HP-COF-1 and HP-COF-2 were estimated to be $V_p = 0.80$ and 1.07 cm^3 g^{-1} at $P/P_0 = 0.99$, respectively. We also measured the CO$_2$ and N$_2$ adsorption isotherms of HP-COFs at 273 K. It shows that HP-COF-1 exhibits a good selectivity for adsorption of CO$_2$ over N$_2$ (24.8, Henry's method)[41] with a CO$_2$ adsorption capacity of 54 cm^3 g^{-1} at 1 atm. HP-COF-2 shows lower CO$_2$ adsorption capacity (37 cm^3 g^{-1} at 1 atm),
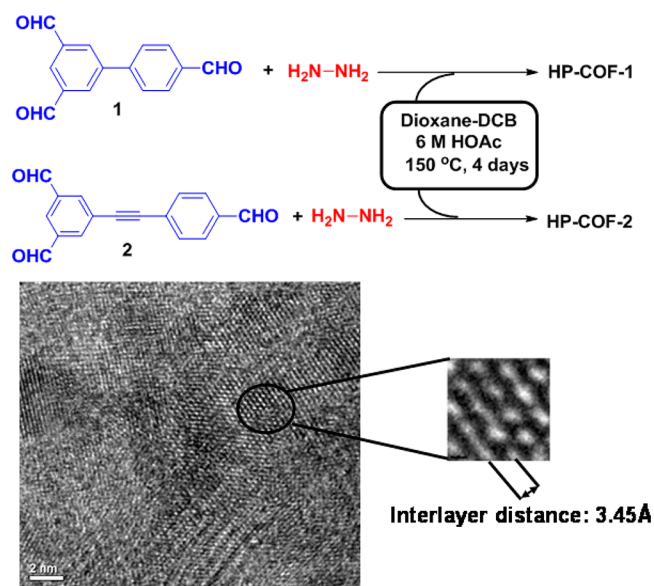

Figure 1. Syntheses of HP-COFs and TEM image of HP-COF-1. The scale bar is 2 nm.

however, with significantly enhanced CO$_2$/N$_2$ adsorption selectivity (41.6). The estimated heats of adsorption of HP-COF-1 and HP-COF-2 were calculated based on the CO$_2$ adsorption isotherms at different temperatures (Virial's method),[42] which, respectively, show similar values of 31.5 and 32.4 kJ·mol^{-1} at zero coverage. These values are comparable with the recently published azine linked COFs.[43]

The crystallinities of HP-COF-1 and HP-COF-2 were determined by PXRD analysis. The diffraction data clearly indicate the crystalline feature of HP-COF-1 and HP-COF-2. Higher-quality diffraction data were obtained for HP-COF-1 (Figure 2a), which was indexed on the basis of a primitive hexagonal lattice. We observed diffraction peaks of HP-COF-1 at 5.12° and 8.30°, which can be assigned to the 110 and 210 plane diffraction, respectively. In addition, a peak at 25.56°
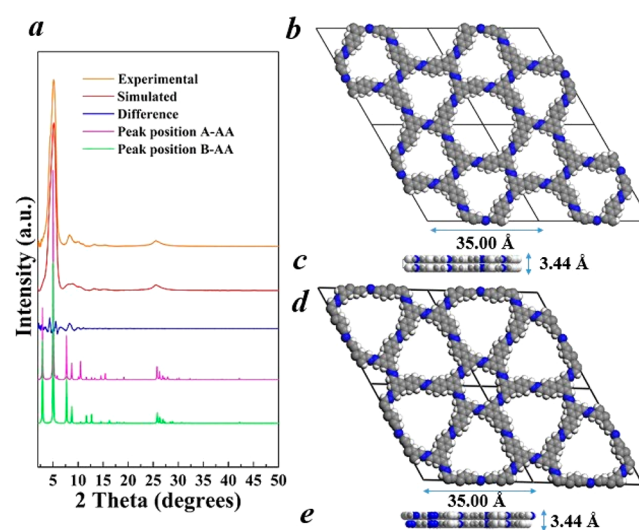

Figure 2. (a) PXRD patterns of HP-COF-1; (b,c) the unit cell structure of isomer A of HP-COF-1 in AA stacking, top view (b) and the view along the *Z* axis (c); (d,e) the unit cell structure of isomer B of HP-COF-1 in AA stacking, top view (d) and the view along the *Z* axis (e).
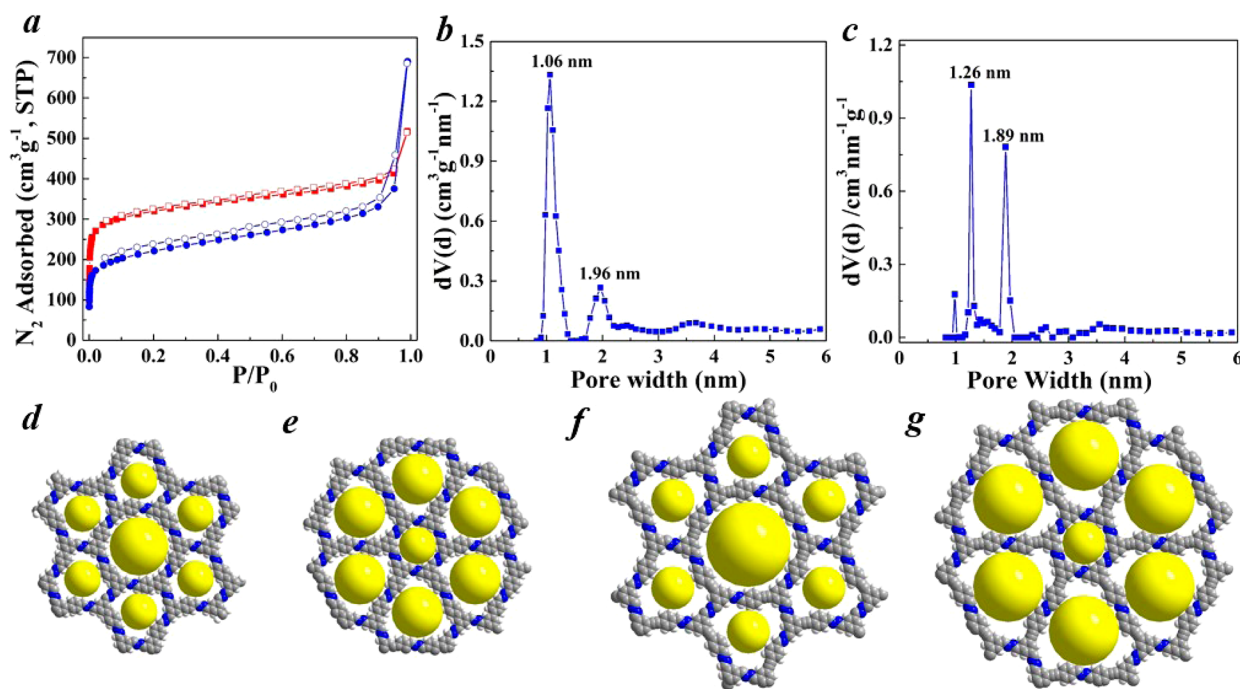
Figure 3. (a) N_2 adsorption and desorption isotherms of HP-COF-1 (red) and HP-COF-2 (blue); (b,c) PSDs of HP-COF-1 (b) and HP-COF-2 (c); (d,e) the pore structure models of HP-COF-1: isomer A (d) and isomer B (e); (f,g) the pore structure models of HP-COF-2: isomer A (f) and isomer B (g).

correlating to the value of the interlayer distance was observed. The d spacing of HP-COF-1 was calculated to be 3.44 Å, which is consistent with the TEM characterization (Figure 1). We did not observe diffraction peaks that are characteristic for the starting materials. In order to determine the periodic structure, the theoretical simulation study was performed on the hexagonal system, with layers lying on the ab plane. The *Reflex* module in Material Studio software package was used in conjunction with the PXRD data.

It should be noted that the combination of C_{2v} symmetric vertex and linear linker would generate two possible isomers (A and B, Scheme 1c) with symmetric infinite honeycomb periodic structures. Both of them contain two different kinds of hexagonal pores. We evaluated these two possible isomers in both the AA stacking and AB stacking modes (Figures 2 and S3). A geometrical energy minimization was performed, using the universal force-field implemented in the *forcite* module, to optimize the geometry of the building blocks as well as the unit cell parameters. We found HP-COF-1 in AB stacking mode has significantly higher total energies (273.19 and 267.67 kcal/mol, respectivel,y for isomers A and B) compared to the values calculated for AA stacking models (117.19 and 117.16 kcal/mol for isomers A and B), indicating AA stacking is energetically more favored. In addition, the observed interlayer distance (3.44 Å) agrees better with calculated distance of 3.45 Å for AA stacking model rather than that (3.31 Å) of AB stacking model. Therefore, HP-COF-1 is more likely AA-stacked. A full profile pattern matching (Pawley) refinement in the *Reflex* module produced unit cell parameters for HP-COF-1 in AA stacking mode: $a = b = 35.00$ Å, $c = 3.44$ Å (residuals: $R_p = 9.76\%$ and $R_{wp} = 5.14\%$); and HP-COF-2: $a = b = 39.89$ Å, $c = 3.47$ Å (residuals: $R_p = 1.92\%$ and $R_{wp} = 1.47\%$), which agree well with the observed reflections. The same unit cell parameters were obtained for both isomers of HP-COF-1 and HP-COF-2 in AA stacking. The powder diffraction patterns for the models were

then calculated and compared with the experimental ones. We found the simulated PXRD patterns of both isomers of HP-COF-1 are in agreement with experimental results, further supporting the eclipsed AA stacking of the layers (Figure 2). It should be noted that the 100 diffraction peak, which is shown at 2.92° in the simulated PXRD for AA stacking model of HP-COF-1, was not observed experimentally. As shown in the simulated PXRD patterns of HP-COF-1, 100 diffraction is not the strongest peak, which is in great contrast to the commonly observed diffraction patterns of highly regular COFs with uniform pore structures. Presumably, the heterogeneous pore structure in HP-COF-1 decreases the regularity of pore distribution and spacing, thus leading to possible broadening/disappearance of the 100 diffraction peak.

Since isomers A and B have similar cell parameters and simulated diffraction patterns, in order to assign the exact isomer structure, we performed the pore size distribution (PSD) analysis of these COFs using nonlocal density functional theory (NL-DFT) model (Figure 3, Table 1). It reveals that

Table 1. Gas Adsorption Properties and Pore Size Distributions of HP-COFs

COFs	SA_{BET}[a]	V_{total}[b]	pore size (nm)		
			predicted[c]		
			isomer A	isomer B	experimental[d]
HP-COF-1	1197	0.80	1.11, 1.93	1.08, 1.56	1.06, 1.96
HP-COF-2	804	1.07	1.16, 2.34	1.09, 1.81	1.26, 1.89

[a]Surface area ($m^2 \cdot g^{-1}$) calculated from the nitrogen adsorption based on the BET models. [b]Total pore volumes ($cm^3 \cdot g^{-1}$) calculated at $P/P_0 = 0.99$. [c]Predicted pore sizes based on the eclipsed stacking of layers. [d]Calculated pore sizes from nitrogen adsorption isotherms using NL-DFT-N_2-carbon adsorption branch kernel at 77 K based on a slit/cylindrical pore model.

HP-COF-1 exhibits two major pores around 1.06 and 1.96 nm, with greater abundance of smaller pores. The experimental result thus agrees better with the simulated isomer A, in which one large pore with the size of 1.93 nm is surrounded by six small pores with the size of 1.11 nm. For HP-COF-2, the PSD analysis shows two major peaks around 1.26 and 1.89 nm with more abundant larger pores. These results suggest the formation of isomer B in the case of HP-COF-2, whose simulated structure shows two pores of sizes around 1.09 and 1.81 nm (more abundant), closely matching with the experimental result.

In conclusion, we have successfully synthesized two COFs with periodically heterogeneous pore structures through the desymmetrized vertex design strategy. PSD analysis revealed that two distinctive micropores (1.06−1.96 nm) were incorporated into the resulting COFs. The structure assignment is supported by PXRD analysis, theoretical simulation, and the PSD experimental data. Our design strategy is generally applicable and opens new possibilities for developing COFs with heterogeneous pore structures targeting specified material properties.

■ ASSOCIATED CONTENT

Ⓢ Supporting Information

The Supporting Information is available free of charge on the ACS Publications website at DOI: 10.1021/jacs.5b09487.

> Detailed synthetic procedure for the preparation of the COFs, FT-IR spectra, solid-state ^{13}C CP-MAS NMR spectrum, TGA graph, SEM and TEM images, additional gas adsorption data, PXRD analysis, and structural simulation (PDF)

■ AUTHOR INFORMATION

Corresponding Author

*wei.zhang@colorado.edu

Notes

The authors declare no competing financial interest.

■ ACKNOWLEDGMENTS

■ REFERENCES

(1) Cote, A. P.; Benin, A. I.; Ockwig, N. W.; O'Keeffe, M.; Matzger, A. J.; Yaghi, O. M. *Science* **2005**, *310*, 1166.
(2) El-Kaderi, H. M.; Hunt, J. R.; Mendoza-Cortes, J. L.; Cote, A. P.; Taylor, R. E.; O'Keeffe, M.; Yaghi, O. M. *Science* **2007**, *316*, 268.
(3) Feng, X.; Ding, X. S.; Jiang, D. L. *Chem. Soc. Rev.* **2012**, *41*, 6010.
(4) Ding, S. Y.; Wang, W. *Chem. Soc. Rev.* **2013**, *42*, 548.
(5) Tilford, R. W.; Mugavero, S. J.; Pellechia, P. J.; Lavigne, J. J. *Adv. Mater.* **2008**, *20*, 2741.
(6) Colson, J. C.; J, W.; Woll, A. R.; Mukherjee, A.; Levendorf, M. P.; Spitler, E. L.; Shields, V. B.; Spencer, M. G.; Park, J.; Dichtel, W. R. *Science* **2011**, *332*, 228.
(7) Kandambeth, S.; Mallick, A.; Lukose, B.; Mane, M. V.; Heine, T.; Banerjee, R. *J. Am. Chem. Soc.* **2012**, *134*, 19524.
(8) Biswal, B. P.; Chandra, S.; Kandambeth, S.; Lukose, B.; Heine, T.; Banerjee, R. *J. Am. Chem. Soc.* **2013**, *135*, 5328.
(9) Han, S. S.; Furukawa, H.; Yaghi, O. M.; Goddard, W. A. *J. Am. Chem. Soc.* **2008**, *130*, 11580.
(10) Furukawa, H.; Yaghi, O. M. *J. Am. Chem. Soc.* **2009**, *131*, 8875.
(11) Ding, S. Y.; Gao, J.; Wang, Q.; Zhang, Y.; Song, W. G.; Su, C. Y.; Wang, W. *J. Am. Chem. Soc.* **2011**, *133*, 19816.
(12) Xu, H.; Chen, X.; Gao, J.; Lin, J. B.; Addicoat, M.; Irle, S.; Jiang, D. L. *Chem. Commun.* **2014**, *50*, 1292.
(13) Wan, S.; Guo, J.; Kim, J.; Ihee, H.; Jiang, D. L. *Angew. Chem., Int. Ed.* **2008**, *47*, 8826.
(14) Wan, S.; Gandara, F.; Asano, A.; Furukawa, H.; Saeki, A.; Dey, S. K.; Liao, L.; Ambrogio, M. W.; Botros, Y. Y.; Duan, X. F.; Seki, S.; Stoddart, J. F.; Yaghi, O. M. *Chem. Mater.* **2011**, *23*, 4094.
(15) DeBlase, C. R.; Silberstein, K. E.; Truong, T. T.; Abruna, H. D.; Dichtel, W. R. *J. Am. Chem. Soc.* **2013**, *135*, 16821.
(16) O'Keeffe, M.; Peskov, M. A.; Ramsden, S. J.; Yaghi, O. M. *Acc. Chem. Res.* **2008**, *41*, 1782.
(17) Jin, Y. H.; Yu, C.; Denman, R. J.; Zhang, W. *Chem. Soc. Rev.* **2013**, *42*, 6634.
(18) Liu, X. H.; Guan, C. Z.; Ding, S. Y.; Wang, W.; Yan, H. J.; Wang, D.; Wan, L. J. *J. Am. Chem. Soc.* **2013**, *135*, 10470.
(19) Yue, J. Y.; Liu, X. H.; Sun, B.; Wang, D. *Chem. Commun.* **2015**, *51*, 14318.
(20) Sai, H.; Tan, K. W.; Hur, K.; Asenath-Smith, E.; Hovden, R.; Jiang, Y.; Riccio, M.; Muller, D. A.; Elser, V.; Estroff, L. A.; Gruner, S. M.; Wiesner, U. *Science* **2013**, *341*, 530.
(21) Seo, M.; Kim, S.; Oh, J.; Kim, S. J.; Hillmyer, M. A. *J. Am. Chem. Soc.* **2015**, *137*, 600.
(22) Ning, Y.; Yang, Y.; Wang, C. Y.; Ngai, T.; Tong, Z. *Chem. Commun.* **2013**, *49*, 8761.
(23) Wong-Foy, A. G.; Lebel, O.; Matzger, A. J. *J. Am. Chem. Soc.* **2007**, *129*, 15740.
(24) Schnobrich, J. K.; Lebel, O.; Cychosz, K. A.; Dailly, A.; Wong-Foy, A. G.; Matzger, A. J. *J. Am. Chem. Soc.* **2010**, *132*, 13941.
(25) Xie, Y. B.; Yang, H.; Wang, Z. Y. U.; Liu, Y. Y.; Zhou, H. C.; Li, J. R. *Chem. Commun.* **2014**, *50*, 563.
(26) Fang, Z. L.; Bueken, B.; De Vos, D. E.; Fischer, R. A. *Angew. Chem., Int. Ed.* **2015**, *54*, 7234.
(27) Furukawa, H.; Muller, U.; Yaghi, O. M. *Angew. Chem., Int. Ed.* **2015**, *54*, 3417.
(28) Choi, K. M.; Jeon, H. J.; Kang, J. K.; Yaghi, O. M. *J. Am. Chem. Soc.* **2011**, *133*, 11920.
(29) Zhou, T. Y.; Xu, S. Q.; Wen, Q.; Pang, Z. F.; Zhao, X. *J. Am. Chem. Soc.* **2014**, *136*, 15885.
(30) Feng, X.; Dong, Y. P.; Jiang, D. L. *CrystEngComm* **2013**, *15*, 1508.
(31) Yang, H. S.; Du, Y.; Wan, S.; Trahan, G. D.; Jin, Y. H.; Zhang, W. *Chem. Sci.* **2015**, *6*, 4049.
(32) Baldwin, L. A.; Crowe, J. W.; Shannon, M. D.; Jaroniec, C. P.; McGrier, P. L. *Chem. Mater.* **2015**, *27*, 6169.
(33) Colson, J. W.; Dichtel, W. R. *Nat. Chem.* **2013**, *5*, 453.
(34) Dalapati, S.; Jin, S. B.; Gao, J.; Xu, Y. H.; Nagai, A.; Jiang, D. L. *J. Am. Chem. Soc.* **2013**, *135*, 17310.
(35) Campbell, N. L.; Clowes, R.; Ritchie, L. K.; Cooper, A. I. *Chem. Mater.* **2009**, *21*, 204.
(36) Ritchie, L. K.; Trewin, A.; Reguera-Galan, A.; Hasell, T.; Cooper, A. I. *Microporous Mesoporous Mater.* **2010**, *132*, 132.
(37) Wan, S.; Guo, J.; Kim, J.; Ihee, H.; Jiang, D. L. *Angew. Chem., Int. Ed.* **2009**, *48*, 5439.
(38) Kuhn, P.; Antonietti, M.; Thomas, A. *Angew. Chem., Int. Ed.* **2008**, *47*, 3450.
(39) Rouquerol, J.; Avnir, D.; Fairbridge, C. W.; Everett, D. H.; Haynes, J. H.; Pernicone, N.; Ramsay, J. D. F.; Sing, K. S. W.; Unger, K. K. *Pure Appl. Chem.* **1994**, *66*, 1739.
(40) Li, Z. P.; Feng, X.; Zou, Y. C.; Zhang, Y. W.; Xia, H.; Liu, X. M.; Mu, Y. *Chem. Commun.* **2014**, *50*, 13825.
(41) Zhou, D. D.; He, C. T.; Liao, P. Q.; Xue, W.; Zhang, W. X.; Zhou, H. L.; Zhang, J. P.; Chen, X. M. *Chem. Commun.* **2013**, *49*, 11728.
(42) Zhu, Y. L.; Long, H.; Zhang, W. *Chem. Mater.* **2013**, *25*, 1630.
(43) Li, Z. P.; Zhi, Y. F.; Feng, X.; Ding, X. S.; Zou, Y. C.; Liu, X. M.; Mu, Y. *Chem. - Eur. J.* **2015**, *21*, 12079.